No.114 **Apr. 2023**

Variable Star Bulletin

SDSS J094002.56+274942.0: an SU UMa star with an orbital period of 3.92 hours and an apparently unevolved secondary

Taichi Kato[1], Tonny Vanmunster[2]

[1] Department of Astronomy, Kyoto University, Sakyo-ku, Kyoto 606-8502, Japan
tkato@kusastro.kyoto-u.ac.jp

[2] Center for Backyard Astrophysics Belgium, Walhostraat 1A, B-3401 Landen, Belgium
tonny.vanmunster@gmail.com

Received 2023 Apr. 25

Abstract

We found that SDSS J094002.56+274942.0 underwent a superoutburst in 2019 February based on our observations and Zwicky Transient Facility (ZTF) data. This object showed shallow eclipses during this superoutburst and we established the orbital period to be 0.1635015(1) d in combination with the ZTF and Asteroid Terrestrial-impact Last Alert System (ATLAS) data in quiescence. Superhumps apparently started to develop soon after the object reached the plateau phase and fully grown superhumps were recorded within the initial 6 d of the plateau phase. Using the superhump and orbital periods, we obtained a mass ratio (q) of 0.39(3) and obtained an inclination of 70.5(5)° by eclipse modeling. These values reproduced the quiescent ellipsoidal variations very well. Using the Gaia parallax and 2MASS observations, we confirmed that the secondary is indistinguishable from an unevolved main-sequence star. The resultant mass ratio and orbital period were the highest among SU UMa stars, and this provided a proof that the 3:1 resonance can develop in less than 6 d even in q=0.39(3). The superoutburst faded relatively rapidly and was followed by a rebrightening, suggesting that the tidal effect in a large-q system was insufficient to maintain a long superoutburst and the remnant matter caused a rebrightening. The presence of such a system among dwarf novae is against the conventional idea that outbursts in dwarf novae are not long enough to develop superhumps, in contrast to novalike variables, under a weak tidal effect. The present observation also supports that the 3:1 resonance is the cause of a long outburst, and not its consequence, even under extreme q. The rapid growth of the 3:1 resonance in a high-q system challenges the generally accepted results of hydrodynamic simulations.

1 Introduction

SU UMa-type dwarf novae are a class of cataclysmic variables (CVs) which show superhumps during long, bright outbursts (superoutbursts) [For general information of CVs and subclasses, see e.g., Warner (1995)]. This phenomenon is widely believed to be the consequence of the 3:1 resonance (Whitehurst 1988; Hirose and Osaki 1990; Lubow 1991) when the disk expands to this radius during a superoutburst. Whether the 3:1 resonance is the cause or the consequence of a superoutburst has been discussed, and a series of analyses of the Kepler data of V1504 Cyg and V344 Lyr (Osaki and Kato 2013a,b, 2014) established that the 3:1 resonance is the cause of a superoutburst as originally proposed by Osaki (1989).

The size of the accretion disk is limited by tidal truncation, or in extreme cases, could be by the size of the Roche lobe. The size of the Roche lobe is a function of the mass ratio $q = M_1/M_2$ and it has long been discussed, both observationally and theoretically, what is the upper limit of q that enables the 3:1 resonance. Numerical simulations such as by smoothed particle hydrodynamics (SPH) gave a limit of q <0.25–0.33 (e.g. Whitehurst and King 1991; Murray 1998; Murray et al. 2000; Smith et al. 2007). CVs with longer orbital periods ($P_{\rm orb}$) have larger q and there is a natural upper limit for $P_{\rm orb}$ for objects showing superhumps. The limit q=0.25 generally corresponds to the period gap in CVs. This limit originally appeared to fit SU UMa-type dwarf novae very well, among which systems above the period gap were very exceptional. It has been well-known, however, superhumps

are present in longer-$P_{\rm orb}$ systems in novalike variables (systems with a thermally stable high-state disk), such as in Bruch (2022); Stefanov et al. (2022); Bruch (2023) using modern Transiting Exoplanet Survey Satellite (TESS: Ricker et al. 2015) data. Although the case of RZ Gru ($P_{\rm orb}$=0.4563 d) in Bruch (2022) may be exceptional and it may have shown a phenomenon different from (ordinary) superhumps, many novalike variables are known to show superhumps at least up to $P_{\rm orb}$=0.18 d (Bruch 2023). Since the majority of long-$P_{\rm orb}$ systems showing superhumps are novalike systems, there has been an idea that a weaker effect of a resonance requires longer time to develop, and systems in high states for a sufficiently long time (i.e. novalike variables) only can show superhumps. In this interpretation, the high states (outbursts) in dwarf novae are not long enough to develop superhumps, somewhat in line with the above-mentioned idea that the 3:1 resonance is the consequence of a long outburst, not the cause.

In recent years, however, a number of SU UMa-type dwarf novae have been discovered above the period gap. The only traditionally known system was TU Men (Stolz and Schoembs 1984)[1]. The q value for TU Men, however, is unfortunately not well-determined (Smak 2006). There is evidence for CNO-processing in this object (Godon and Sion 2021) and TU Men may not be considered an ordinary CV following the standard evolutionary track. Modern examples without evidence of an evolved secondary include CRTS J035905.9+175034 [q=0.281(15): Littlefield et al. (2018)] and BO Cet [q=0.31–0.34: Kato et al. (2021); Kato (2023a)]. Superhumps in both objects started to develop soon after superoutbursts reached the plateau phase as in other SU UMa stars (Osaki and Kato 2013a). There was no indication of a significant delay in the development of superhumps, which would be expected if the 3:1 resonance is the consequence of a long outburst.

SDSS J094002.56+274942.0 was spectroscopically selected as a CV (Szkody et al. 2007). The spectrum by Szkody et al. (2007) was that of an ordinary dwarf nova. Krajci and Wils (2010) noticed an outburst detected by Catalina Real-Time Transient Survey (CRTS) in 2009 and performed time-resolved photometry. Krajci and Wils (2010) detected orbital modulations (ellipsoidal variations) with a period of 0.16352 d during the fading part of this outburst. Although Krajci and Wils (2010) suggested that the disk or the hot spot may have been (partially) eclipsed during the brighter stages of this outburst, the nature of the observed dip was unclear due to the poor phase coverage. Krajci and Wils (2010) discussed that TiO bands expected from the secondary type (M4–5) were invisible in the spectrum of Szkody et al. (2007). Krajci and Wils (2010) noted a possibility of an early M-type secondary, which would suggest an evolved core, with little TiO absorption. Based on this identification of $P_{\rm orb}$, SDSS J094002.56+274942.0 has long been regarded as an SS Cyg-type dwarf nova. Hou et al. (2020) observed this object three times by the LAMOST survey. No CIII/NIII emission lines were recorded. FeII emission lines were recorded once and Hα lines was double-peaked on a single occasion. All spectra were obtained in quiescence and one of them was presented in Han et al. (2020).

During an inspection of Zwicky Transient Facility (ZTF: Masci et al. 2019)[2] data, one of the authors (T.K.) noted that ZTF incidentally obtained time-resolved photometry during a long outburst in 2019 February. Combined with time-resolved observations by the second author (T.V.) reported to VSNET Collaboration (Kato et al. 2004), T.K. found that this outburst was a superoutburst and that this object showed superhumps (vsnet-chat 9373)[3].

2 Data analysis

The observations by T.V. were obtained with a 0.40-m f/5.1 Newton telescope and an unfiltered Starlight Xpress Trius SX-46 CCD camera with KAF-16200 (3×3 bin) chip, located in Extremadura, Spain. We used ZTF and Asteroid Terrestrial-impact Last Alert System (ATLAS: Tonry et al. 2018) forced photometry (Shingles et al. 2021) data for our analysis. Some unfiltered snapshot observations reported to VSOLJ were also used (hereafter CCD). Some ATLAS and CCD observations had false bright detections, which were removed after comparison with the observations on the same night or with other observers. Although TESS also observed this object in quiescence, these observations were strongly contaminated by nearby brighter stars and we did not use them since they were not particularly useful in determining $P_{\rm orb}$ in the presence of ZTF and ATF observations with a longer baseline. The log of time-resolved observations is listed in table 1. When analyzing the quiescent data, we

[1]The case of U Gem was claimed by Smak and Waagen (2004), but T.K. considered it questionable (Kato et al. 2014b) and the case is far from being established [see also Patterson et al. (2005)].

[2]The ZTF data can be obtained from IRSA <https://irsa.ipac.caltech.edu/Missions/ztf.html> using the interface <https://irsa.ipac.caltech.edu/docs/program_interface/ztf_api.html> or using a wrapper of the above IRSA API <https://github.com/MickaelRigault/ztfquery>.

[3]<http://ooruri.kusastro.kyoto-u.ac.jp/mailarchive/vsnet-chat/9373>.

Table 1: Time-resolved photometry of SDSS J094002.56+274942.0.

Start*	End*	Mean mag.	Error	$N^\dagger$	Observer	Filter
58522.3249	58522.5274	14.600	0.004	95	Vanmunster	CV
58523.3216	58523.4898	14.742	0.006	41	Vanmunster	CV
58523.7527	58523.9151	14.688	0.007	56	ZTF	r
58524.4699	58524.4930	14.815	0.003	28	Vanmunster	CV
58524.7530	58524.9168	14.782	0.006	57	ZTF	r
58526.3213	58526.5304	15.030	0.006	245	Vanmunster	CV
58526.7307	58526.8945	14.936	0.011	57	ZTF	r

*BJD−2400000.

†Number of observations.

used locally-weighted polynomial regression (LOWESS: Cleveland 1979) to remove long-term trends. The periods were determined using the phase dispersion minimization (PDM: Stellingwerf 1978) method, whose errors were estimated by the methods of Fernie (1989); Kato et al. (2010).

3 Results

3.1 Long-term behavior

Long-term light curves are shown in figures 1 and 2. This object showed outbursts relatively infrequently. The 2019 February outburst (fourth panel in figure 1) was a long one, which later turned out to be a superoutburst (subsection 3.3), while the other three were short. The 2009 outburst observed by Krajci and Wils (2010) was also a short one. The rarity of outbursts suggests a low mass-transfer rate.

The details of the 2019 February long outburst are shown in figure 3. This outburst had an approximate duration of 20 d and was followed by a rebrightening on 2019 March 3 (BJD 2458546). The overall shape of this outburst is compatible with that of a superoutburst, which will be examined in subsection 3.3.

3.2 Orbital period and profile

We used ZTF and ATLAS observations in quiescence (all bands were combined after zero-point adjustments) and obtained the same ellipsoidal variations detected by Krajci and Wils (2010) (figure 4). The orbital phase was defined by

$$\mathrm{Min(BJD)} = 2458953.7169(10) + 0.1635015(1)E. \quad (1)$$

The zero phase was determined by an MCMC analysis (Kato et al. 2010) of the eclipses detected during the 2019 superoutburst (see subsection 3.3) since eclipses during an outburst are a better indicator of the center of the disk particularly when a hot spot is present. This ephemeris, however, very well expressed the primary (but shallower) minimum of the ellipsoidal variations in quiescence. The phase 0.75 peak was brighter than the phase 0.25 one probably due to the hot spot. The secondary (but deeper) minimum occurred somewhat before the phase 0.5.

3.3 Eclipses and superhumps in superoutburst

We show phase-averaged light curves during the 2019 February outburst in figure 5. The orbital phases were obtained using equation (1). The four runs (ZTF and the final night by Vanmunster) were slightly longer than P_{orb} and full orbital phases were sampled in these cases. This figure corresponds to figure 3 in Krajci and Wils (2010) (but phase-averaged). Eclipses were present in all runs covering the expected eclipse phase and we used these data to determine the zero phase of equation (1). The eclipses became asymmetric during the third and fifth runs, probably reflecting the evolution of superhumps. In the sixth and seventh runs, the presence of superhumps having a period longer than P_{orb} is apparent. The result of a PDM analysis of the combined sixth and seventh runs is shown in figure 6 after removing the eclipse parts (phases within ± 0.06). There was some ambiguity in the difference in the zero points between these two runs (they were by different observers using different equipment

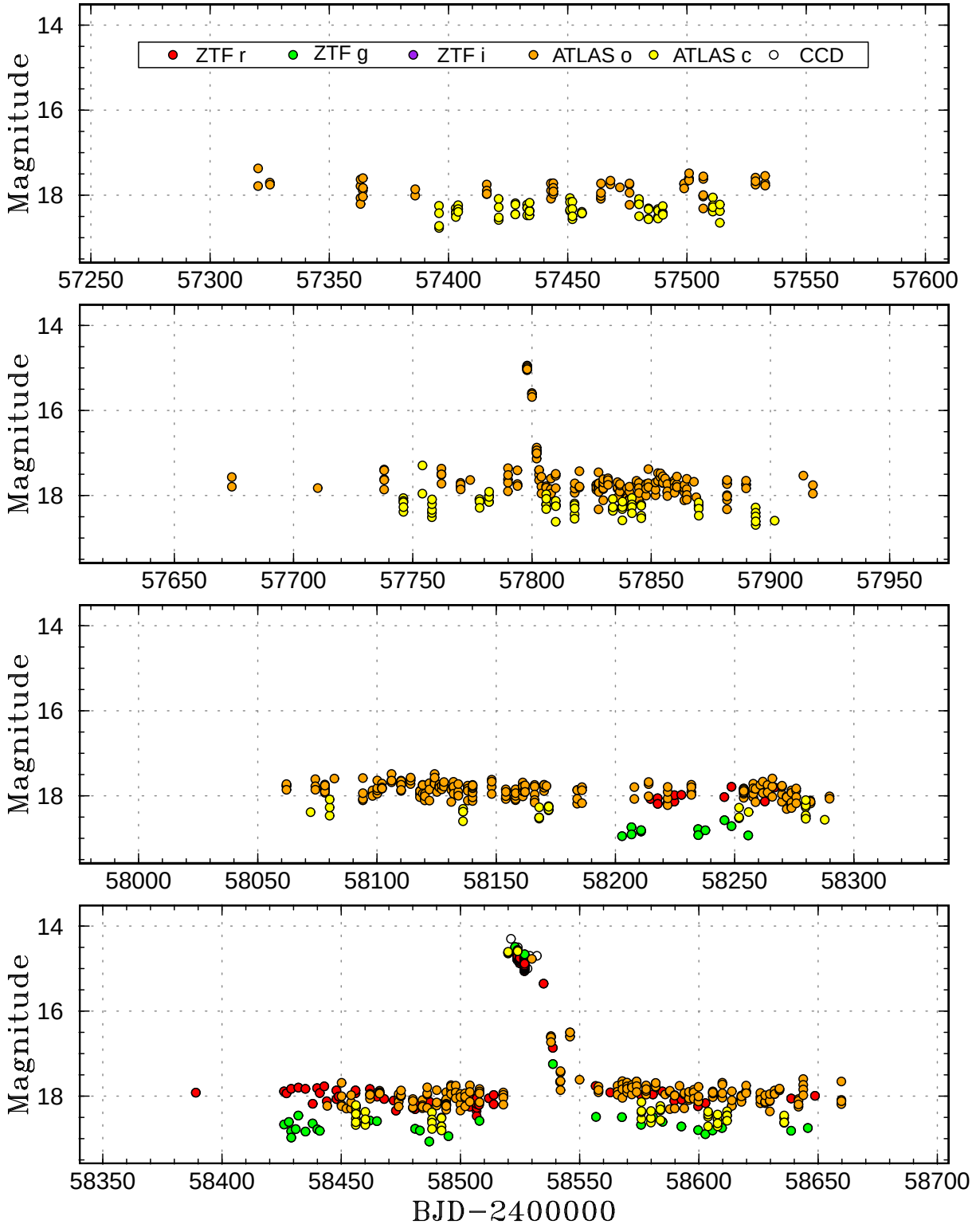

Figure 1: Light curve of SDSS J094002.56+274942.0 in 2015–2019. CCD refers to unfiltered snapshot observations.

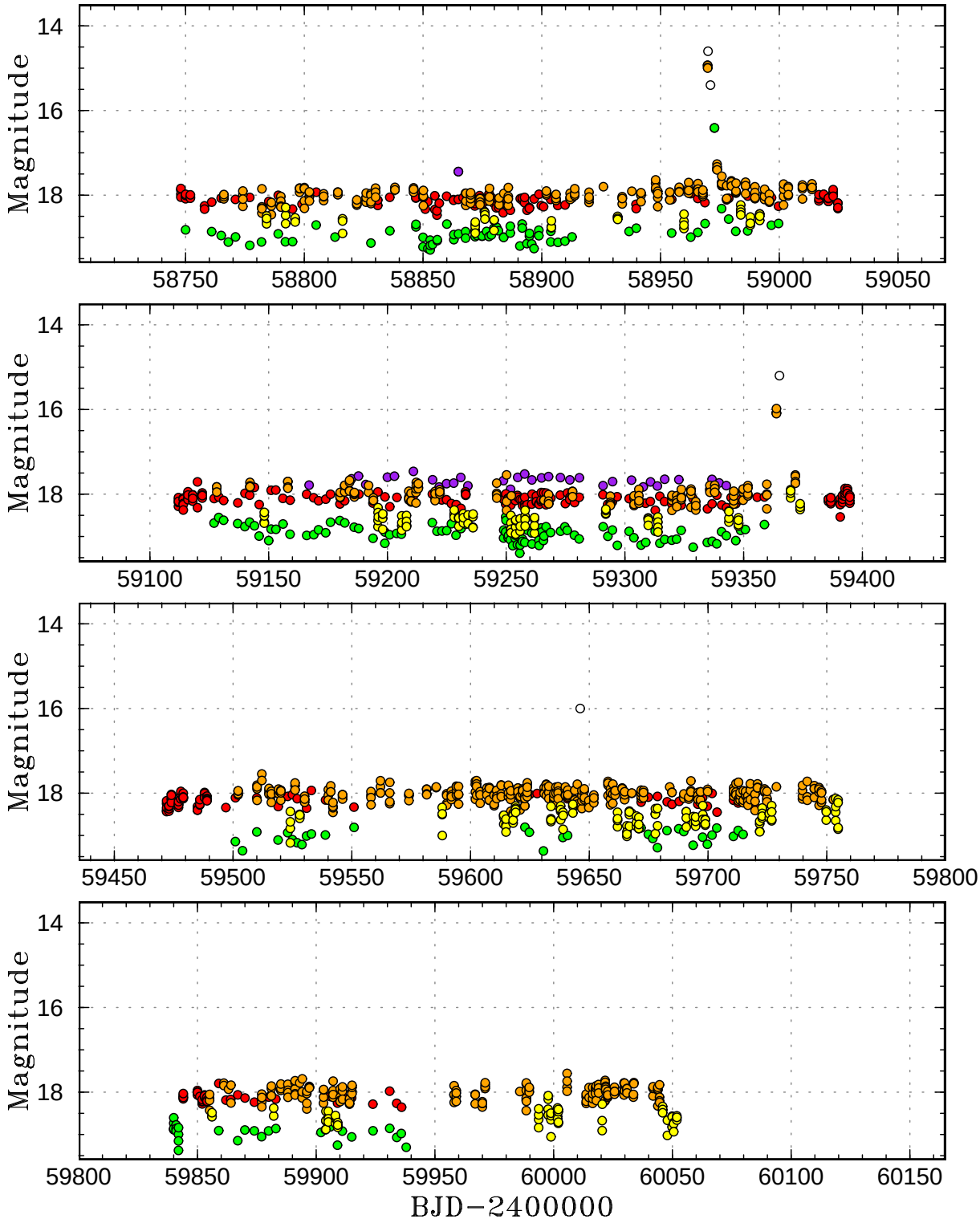

Figure 2: Light curve of SDSS J094002.56+274942.0 in 2019–2023. The symbols are the same as in figure 1.

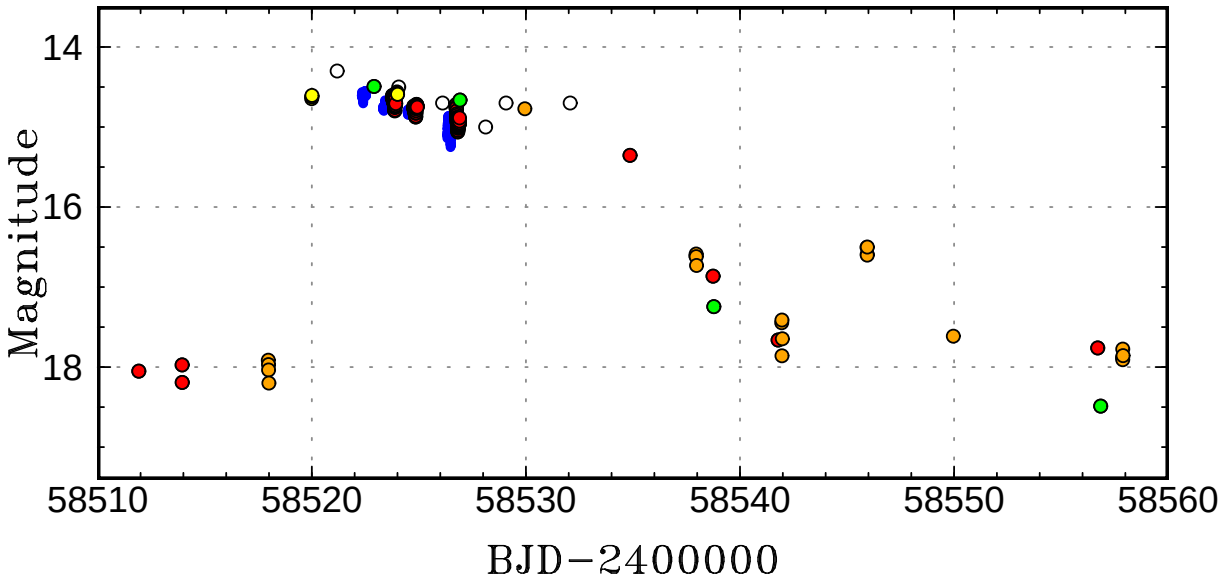

Figure 3: Light curve of SDSS J094002.56+274942.0 during the 2019 February superoutburst. Blue plots are time-resolved photometry by T.V. The other symbols are the same as in figure 1.

and filters). We adopted a correction of 0.050 mag to the ZTF data so that the maxima and minima of these two runs become the same. This ambiguity, however, did not strongly affect the result. The resultant period was 0.1825(7) d. With this period, the peaks of the superhump maxima from the two sets of the data well agree although the waveforms were somewhat different, probably due to the beat phenomenon between the orbital and superhump periods (figure 6). The nominal (statistical) error could be an underestimate due to a systematic error arising from the beat phenomenon and intrinsic variations. A result from a short (0.57 d) baseline would be more strongly affected by these effects than in ordinary superhump analyses using longer baselines, such as in Kato et al. (2009). We, however, disregard this possibility in the following discussions and use the nominal error.

Although superhumps apparently grew before the sixth run, we could not determine the period before this run partly due to the overlapping orbital signal. There was a gap more than 1 d before the sixth run and it appears that the major increase of the superhump amplitude occurred during this observational gap.

4 Discussion

4.1 Mass ratio and the secondary

With $P_{\rm orb}$ of 0.1635015 d = 3.924 hr, a CV on the standard evolutionary sequence is expected to have a secondary mass of M_2=0.303 $M_\odot$ (main sequence) and near-infrared absolute magnitudes of M_J=6.87, M_H=6.45 and M_K=6.29 (Knigge 2006, 2007). These near-infrared absolute magnitudes can be directly comparable to the observed 2MASS magnitudes (Cutri et al. 2003) and the Gaia parallax yielding a distance modulus of 9.5(2) mag (Gaia Collaboration et al. 2022). The observed J=16.15(11), H=15.61(16) and K_s=15.48(18) correspond to the absolute magnitudes of M_J=6.7(2), M_H=6.1(3) and M_K=6.0(3). These values exclude a possibility of an evolved donor as in other SU UMa stars with very long $P_{\rm orb}$ [such as ASASSN-18aan ($P_{\rm orb}$=0.149454 d, Wakamatsu et al. 2021) and ASASSN-15cm ($P_{\rm orb}$=0.2084652 d, Kato 2023b)]. The secondary star in SDSS J094002.56+274942.0 appears to be indistinguishable from a normal main-sequence star. Assuming a white dwarf with an average mass M_1=0.82$M_\odot$ in short-period CVs (Savoury et al. 2011; Zorotovic et al. 2011; McAllister et al. 2019; Pala et al. 2022), the expected mass of the secondary translates to q=0.37.

What is inferred from the superhump observation? It is well established that superhump periods vary (Kato et al. 2009) and it is important which stage is used for estimating q from the superhump period (Kato and Osaki 2013; Kato 2022a). In the case of SDSS J094002.56+274942.0, the superhump observations were apparently made just around the peak of the superhump amplitude. It is known that stage A–B transition [see Kato et al. (2009); Kato (2022b) for superhump stages] does not match the peak of the superhump amplitude in long-$P_{\rm orb}$

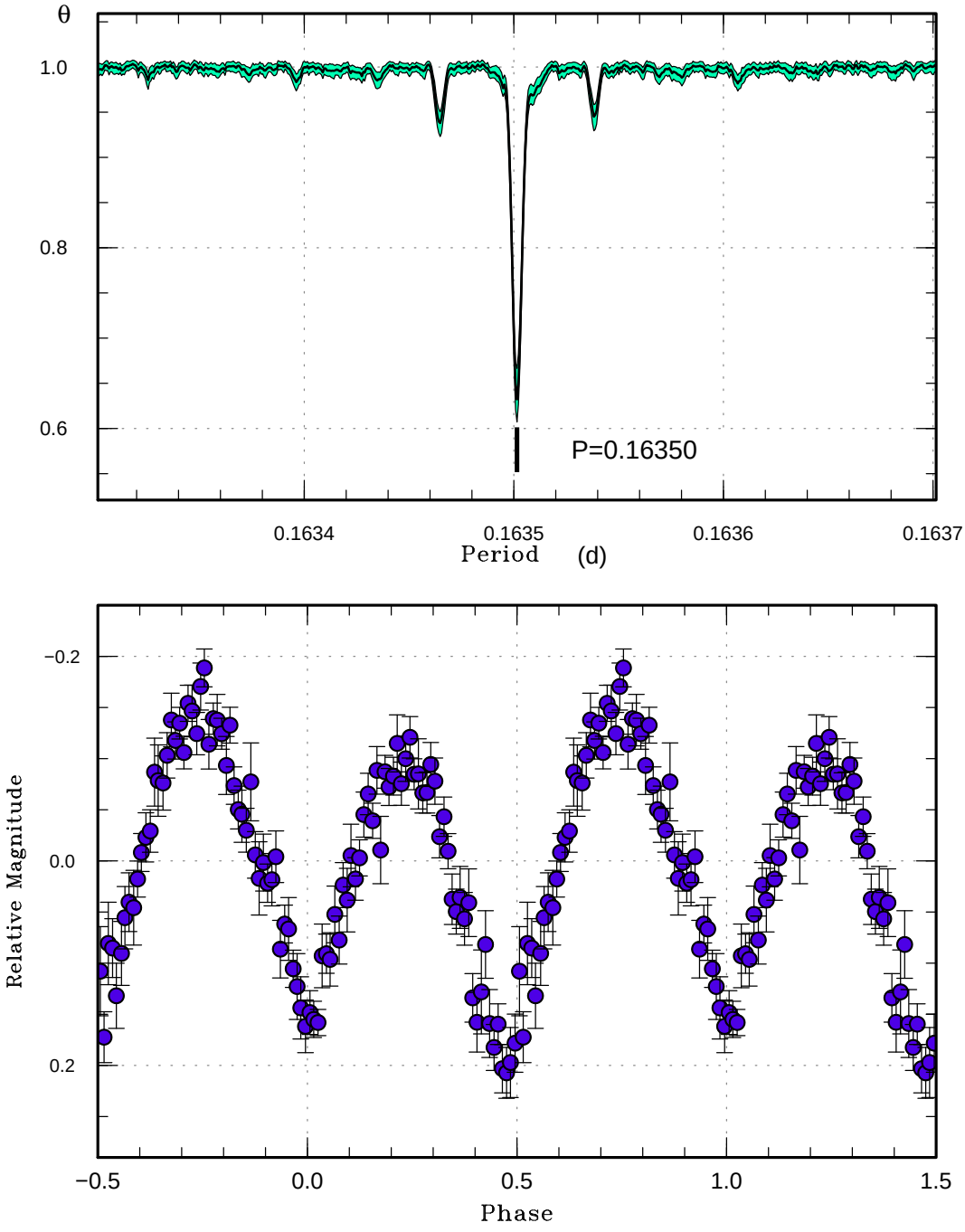

Figure 4: Orbital profile of SDSS J094002.56+274942.0 in quiescence. (Upper): PDM analysis. The bootstrap result using randomly contain 50% of observations is shown as a form of 90% confidence intervals in the resultant θ statistics. (Lower): Phase plot.

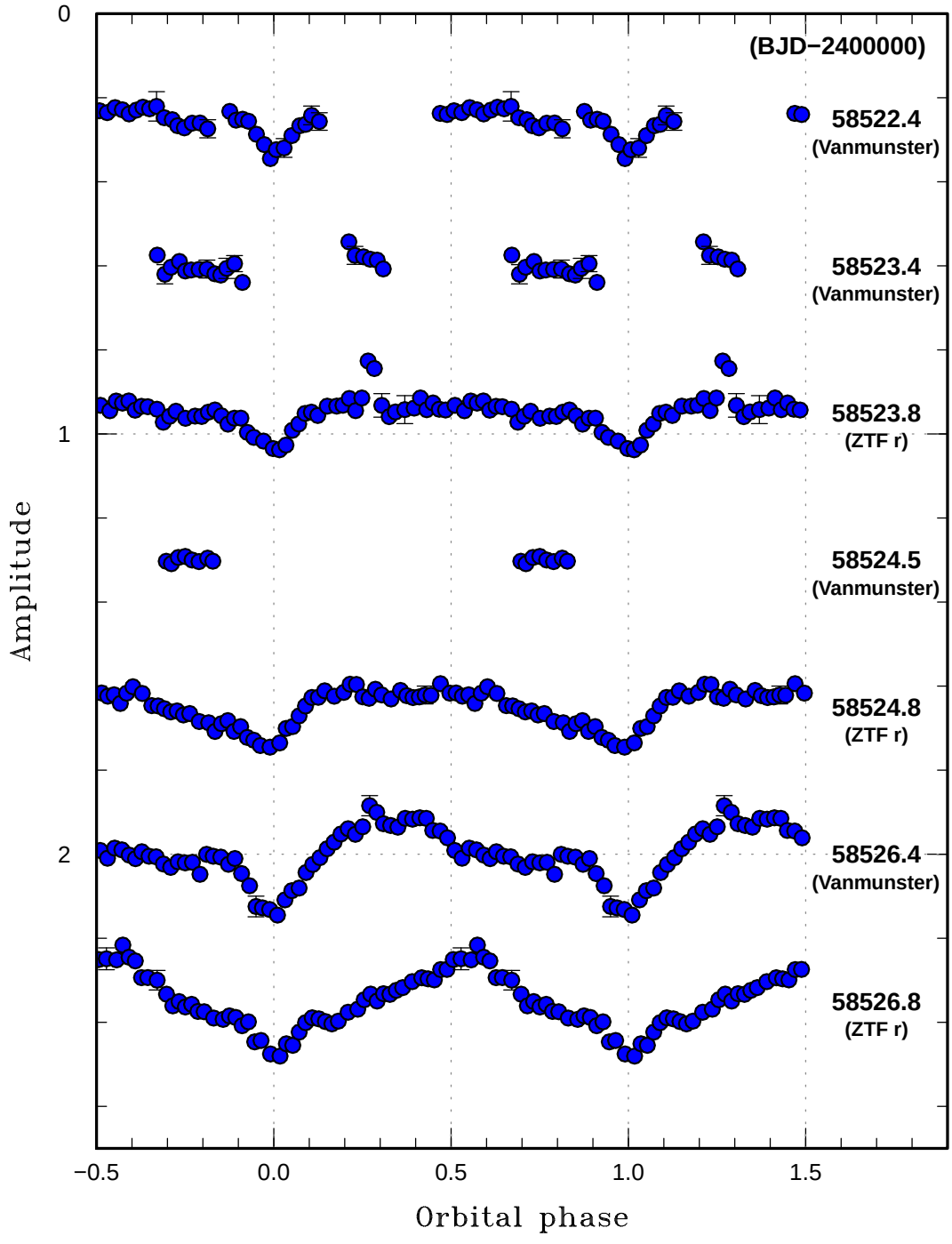

Figure 5: Phased profiles during the 2019 February superoutburst. The orbital phase is defined by equation (1). The values to the right refer to the center of observational runs.

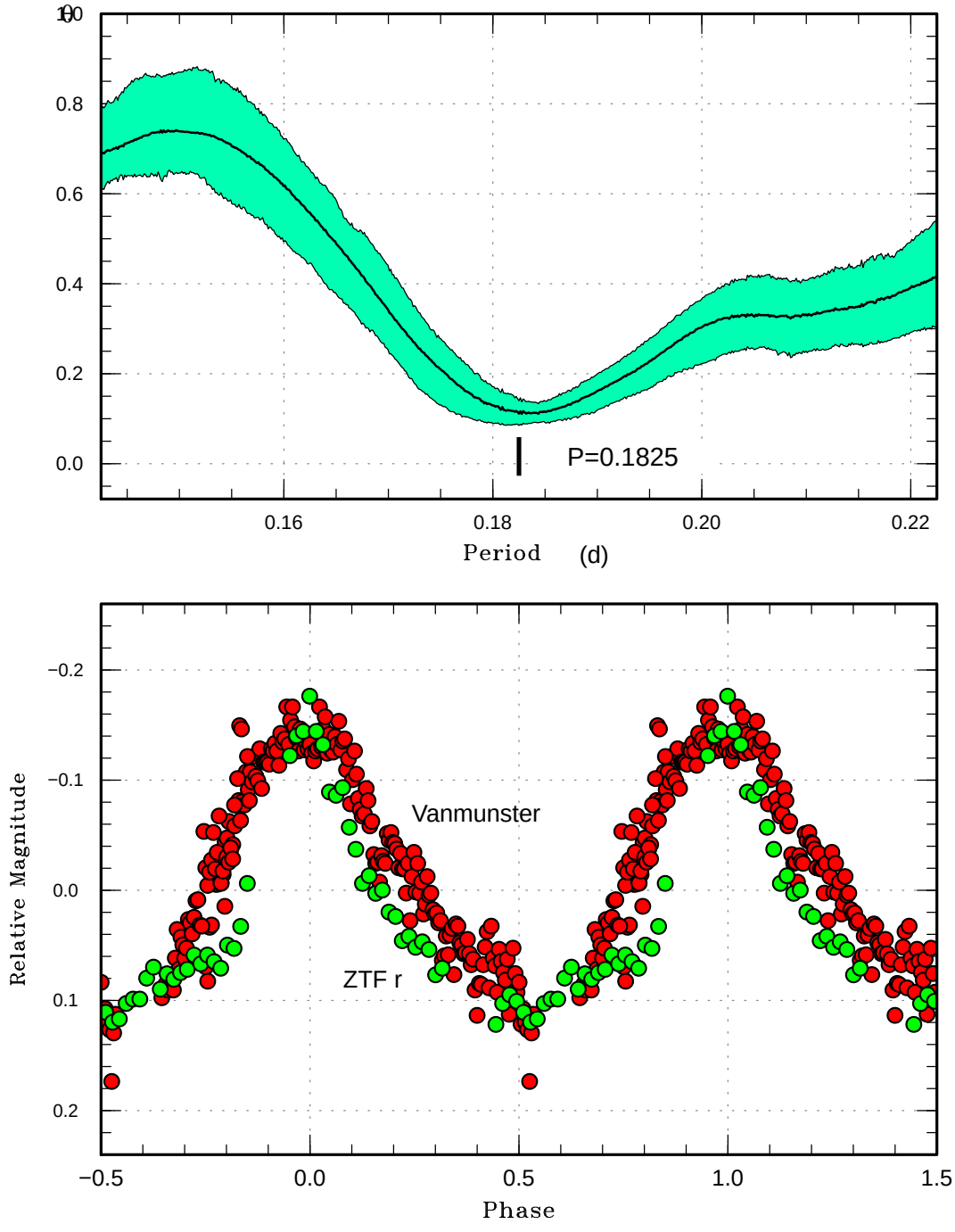

Figure 6: Superhumps in SDSS J094002.56+274942.0. The data for BJD 2458526.33–2458526.90 were used after removing eclipse parts. (Upper): PDM analysis. (Lower): Phase plot.

Table 2: Eclipse modeling during superoutburst.

q	Inclination (°)
0.37	71.0
0.39	70.5
0.42	70.0

systems and stage A (judged from the superhump period) extends slight after the maximum of the superhump amplitude [V1006 Cyg: Kato et al. (2016, see supplementary figure) and MN Dra: Kato et al. (2014a)]. We therefore consider that the superhump period ($P_{\rm SH}$) recorded in SDSS J094002.56+274942.0 reflects that of stage A superhumps. The observed $\epsilon^* \equiv 1 - P_{\rm orb}/P_{\rm SH}$ was 0.104(4). This corresponds to q=0.39(3) [see table 1 in Kato (2022a)]. Considering the uncertainty in determining the superhump period and an assumption of the white dwarf mass, this value appears to be consistent with a normal main-sequence secondary. The superhump period at least does not favor a light-weight secondary with an evolved core (as already confirmed by the near-infrared absolute magnitudes).

4.2 Inclination and ellipsoidal variations

Eclipses observed during the superoutburst provide an excellent opportunity for modeling the binary since the disk radius is expected to be the radius of the 3:1 resonance. Assuming an optically thick standard disk, inclinations needed to reproduce the observed eclipse depth (0.11 mag) are given in table 2. We used three q values (0.37 from the standard evolutionary sequence and an average-mass white dwarf, 0.39 from stage A superhumps and 0.42 as the upper limit). The uncertainties of inclinations were 0.5° and the values were rounded to 0.5°.

We followed the case of ASASSN-15cm (Kato 2023b) in modeling the quiescent light curve. Using Ellipsoidal Modulation Light Curve Generator by M. Uemura (2006), which was based on Orosz and Bailyn (1997a,b), we could reproduce ellipsoidal variations ZTF r and g observations in figure 7. We used $T_{\rm eff}$=3500 K, $\log g$=4.727, assuming a main-sequence secondary in Knigge (2006, 2007) and gravity darkening and limb-darkening coefficients given in Claret and Bloemen (2011) (solar metallicity and a microturbulent velocity of 2 km s^{-1} as typical values were used). As in the case of ASASSN-15cm, outbursts in SDSS J094002.56+274942.0 were rare and the mass-transfer rate is expected to be low. The contribution from the disk appears to be negligible in quiescence. Both q=0.37 and q=0.42 cases sufficiently fit the observations with the inclinations determined by eclipse analysis. It turned out that quiescent ellipsoidal variations could not constrain the binary parameter better than what we obtained from superhump and eclipse analysis. This result, however, confirmed that our basic picture (unevolved main-sequence secondary) is correct.

4.3 Implications of the present discovery

As stated in section 1, it has long been considered that CVs above the period gap showing superhumps are almost entirely novalike variables with a thermally stable (high-state) disk. It has been considered that superhumps can grow only in such systems in sufficiently long high states under a weaker resonance effect. Indeed, some established SU UMa-type dwarf novae above the period gap have a secondary with an evolved core such as in OT J002656.6+284933 (=CSS101212:002657+284933, $P_{\rm SH}$=0.13225 d: Kato et al. 2017), ASASSN-18aan ($P_{\rm orb}$=0.149454 d: Wakamatsu et al. 2021) and ASASSN-15cm ($P_{\rm orb}$=0.208466 d: Kato 2023b). Wakamatsu et al. (2021) suggested that the 3:1 resonance in long-$P_{\rm orb}$ dwarf novae is more difficult to develop around the stability border than in the case of the 2:1 resonance. The present discovery of an SU UMa-type dwarf nova with $P_{\rm orb}$=0.1635015 d with a normal main-sequence secondary is against this interpretation. Even with q=0.39(3), this dwarf nova apparently started developing superhumps soon after it reached the plateau phase and fully developed superhumps were recorded within 6 d of the start of the plateau phase. This behavior is common to other SU UMa-type dwarf novae and there was no significant difference in the development of superhumps. This case supports the idea that the 3:1 resonance triggered a superoutburst even in this extreme case.

The superoutburst, however, terminated rather quickly and was followed by a rebrightening. These features suggest that the hot state was difficult to maintain by the 3:1 resonance in an extreme q case — a mechanism proposed in V1006 Cyg and CS Ind which simulated a WZ Sge-type phenomenon (Kato et al. 2016, 2019) — and

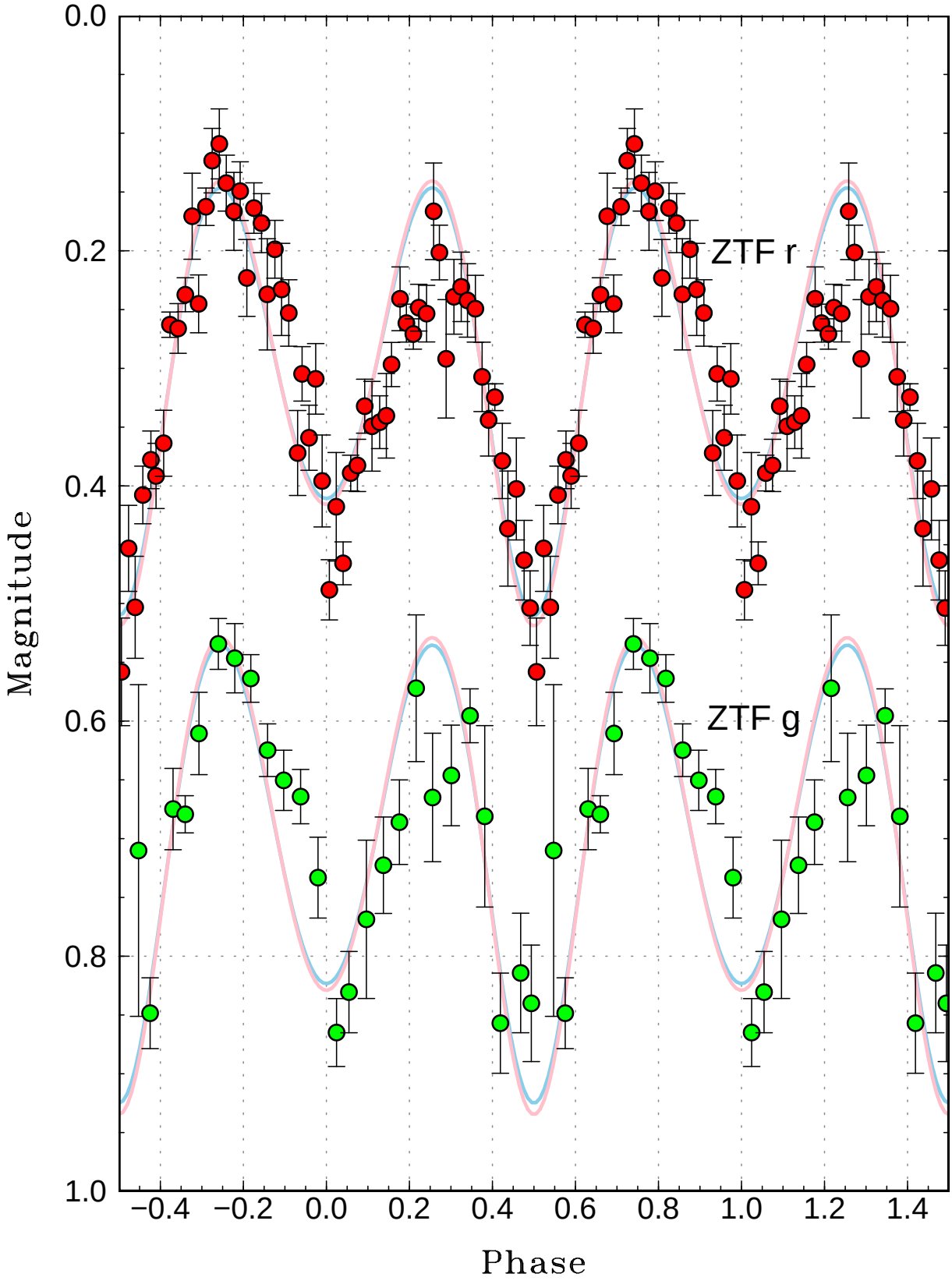

Figure 7: Orbital profile of SDSS J094002.56+274942.0 in quiescence using ZTF r and g data. The orbital phase is defined by equation (1). The plots were shifted by 0.4 mag between different bands. The solid curves represent ellipsoidal variations expected for q=0.43, i=70.0° (skyblue) and q=0.37, i=71.0° (pink) (see text).

that the matter left in the disk due to the early quenching of the superoutburst resulted a rebrightening, which is usually a feature in short-$P_{\rm orb}$ systems (Kato et al. 1998; Kato 2015).

Continued monitoring of this object is required, and better determination of the superhump period and its evolution will clarify what is happening in long-$P_{\rm orb}$ and high-q SU UMa-type dwarf novae.

Acknowledgements

This work was supported by JSPS KAKENHI Grant Number 21K03616. The authors are grateful to the ZTF and ATLAS teams for making their data available to the public. We are grateful to VSOLJ observers (particularly Yutaka Maeda) who reported snapshot CCD photometry of SDSS J094002.56+274942.0. We are also grateful to Makoto Uemura for sharing the code of Ellipsoidal Modulation Light Curve Generator, Naoto Kojiguchi for helping downloading the ZTF and TESS data and Yasuyuki Wakamatsu for converting the data reported to the VSNET Collaboration.

Based on observations obtained with the Samuel Oschin 48-inch Telescope at the Palomar Observatory as part of the Zwicky Transient Facility project. ZTF is supported by the National Science Foundation under Grant No. AST-1440341 and a collaboration including Caltech, IPAC, the Weizmann Institute for Science, the Oskar Klein Center at Stockholm University, the University of Maryland, the University of Washington, Deutsches Elektronen-Synchrotron and Humboldt University, Los Alamos National Laboratories, the TANGO Consortium of Taiwan, the University of Wisconsin at Milwaukee, and Lawrence Berkeley National Laboratories. Operations are conducted by COO, IPAC, and UW.

The ztfquery code was funded by the European Research Council (ERC) under the European Union's Horizon 2020 research and innovation programme (grant agreement n°759194 – USNAC, PI: Rigault).

This work has made use of data from the Asteroid Terrestrial-impact Last Alert System (ATLAS) project. The ATLAS project is primarily funded to search for near earth asteroids through NASA grants NN12AR55G, 80NSSC18K0284, and 80NSSC18K1575; byproducts of the NEO search include images and catalogs from the survey area. This work was partially funded by Kepler/K2 grant J1944/80NSSC19K0112 and HST GO-15889, and STFC grants ST/T000198/1 and ST/S006109/1. The ATLAS science products have been made possible through the contributions of the University of Hawaii Institute for Astronomy, the Queen's University Belfast, the Space Telescope Science Institute, the South African Astronomical Observatory, and The Millennium Institute of Astrophysics (MAS), Chile.

List of objects in this paper

BO Cet, V1006 Cyg, V1504 Cyg, MN Dra, U Gem, RZ Gru, V344 Lyr, TU Men, WZ Sge, SU UMa, ASASSN-15cm, ASASSN-18aan, CRTS J035905.9+175034, CSS101212:002657+284933, OT J002656.6+284933, SDSS J094002.56+274942.0

References

Bruch, A. (2022) TESS light curves of cataclysmic variables – I – Unknown periods in long-known stars. *MNRAS* **514**, 4718

Bruch, A. (2023) TESS light curves of cataclysmic variables – II – Superhumps in old novae and novalike variables. *MNRAS* **519**, 352

Claret, A., & Bloemen, S. (2011) Gravity and limb-darkening coefficients for the *Kepler*, CoRoT, *Spitzer*, *uvby*, *UBVRIJHK*, and Sloan photometric systems. *A&A* **529**, A75

Cleveland, W. S. (1979) Robust locally weighted regression and smoothing scatterplots. *J. Amer. Statist. Assoc.* **74**, 829

Cutri, R. M. et al. (2003) 2MASS All Sky Catalog of point sources (NASA/IPAC Infrared Science Archive)

Fernie, J. D. (1989) Uncertainties in period determinations. *PASP* **101**, 225

Gaia Collaboration et al. (2022) Gaia Data Release 3. Summary of the contents and survey properties. *A&A* **(arXiv:2208.00211)**

Godon, P., & Sion, E. M. (2021) White dwarf photospheric abundances in cataclysmic variables. I. SS Aurigae and TU Mensae. *ApJ* **908**, 173

Han, Z., Boonrucksar, S., Qian, S., Xiaohui, F., Wang, Q., Zhu, L., Dong, A., & Zhi, Q. (2020) Spectroscopic properties of the dwarf nova-type cataclysmic variables observed by LAMOST. *PASJ* **72**, 76

Hirose, M., & Osaki, Y. (1990) Hydrodynamic simulations of accretion disks in cataclysmic variables – superhump phenomenon in SU UMa stars. *PASJ* **42**, 135

Hou, W., Luo, A.-L., Li, Y.-B., & Qin, L. (2020) Spectroscopically identified cataclysmic variables from the LAMOST survey. I. The sample. *AJ* **159**, 43

Kato, T. (2015) WZ Sge-type dwarf novae. *PASJ* **67**, 108

Kato, T. (2022a) Evolution of short-period cataclysmic variables: implications from eclipse modeling and stage a superhump method (with New Year's gift). *VSOLJ Variable Star Bull.* **89**, (arXiv:2201.02945)

Kato, T. (2022b) Analysis of TESS observations of V844 Her during the 2020 superoutburst. *VSOLJ Variable Star Bull.* **102**, (arXiv:2205.05284)

Kato, T. (2023a) SU UMa-type supercycle in the IW And-type dwarf nova BO Cet above the period gap. *VSOLJ Variable Star Bull.* **106**, (arXiv:2302.02593)

Kato, T. (2023b) ASASSN-15cm: an SU UMa star with an orbital period of 5.0 hours. *VSOLJ Variable Star Bull.* **109**, (arXiv:2302.09713)

Kato, T. et al. (2014a) Survey of period variations of superhumps in SU UMa-type dwarf novae. VI: The fifth year (2013–2014). *PASJ* **66**, 90

Kato, T. et al. (2014b) Survey of period variations of superhumps in SU UMa-type dwarf novae. V: The fifth year (2012–2013). *PASJ* **66**, 30

Kato, T., Hambsch, F.-J., Monard, B., Nelson, P., Stubbings, R., & Starr, P. (2019) CS Indi: SU UMa-type dwarf nova with long precursor outburst. *PASJ* **71**, L4

Kato, T. et al. (2009) Survey of period variations of superhumps in SU UMa-type dwarf novae. *PASJ* **61**, S395

Kato, T. et al. (2010) Survey of period variations of superhumps in SU UMa-type dwarf novae. II. The second year (2009–2010). *PASJ* **62**, 1525

Kato, T., Nogami, D., Baba, H., & Matsumoto, K. (1998) in ASP Conf. Ser. 137, Wild Stars in the Old West, ed. S. Howell, E. Kuulkers, & C. Woodward (San Francisco: ASP) p. 9

Kato, T., & Osaki, Y. (2013) New method to estimate binary mass ratios by using superhumps. *PASJ* **65**, 115

Kato, T. et al. (2016) V1006 Cygni: Dwarf nova showing three types of outbursts and simulating some features of the WZ Sge-type behavior. *PASJ* **68**, L4

Kato, T. et al. (2021) BO Ceti: Dwarf nova showing both IW And and SU UMa-type features. *PASJ* **73**, 1280

Kato, T. et al. (2017) OT J002656.6+284933 (CSS101212:002657+284933): An SU UMa-type dwarf nova with longest superhump period. *PASJ* **69**, L4

Kato, T., Uemura, M., Ishioka, R., Nogami, D., Kunjaya, C., Baba, H., & Yamaoka, H. (2004) Variable Star Network: World center for transient object astronomy and variable stars. *PASJ* **56**, S1

Knigge, C. (2006) The donor stars of cataclysmic variables. *MNRAS* **373**, 484

Knigge, C. (2007) Erratum: The donor stars of cataclysmic variables. *MNRAS* **382**, 1982

Krajci, T., & Wils, P. (2010) Photometry of the dwarf nova SDSS J094002.56+274942.0 in outburst. *J. American Assoc. Variable Star Obs.* **38**, 33

Littlefield, C., Garnavich, P., Kennedy, M., Szkody, P., & Dai, Z. (2018) A comprehensive K2 and ground-based study of CRTS J035905.9+175034, an eclipsing SU UMa system with a large mass ratio. *AJ* **155**, 232

Lubow, S. H. (1991) A model for tidally driven eccentric instabilities in fluid disks. *ApJ* **381**, 259

Masci, F.-J. et al. (2019) The Zwicky Transient Facility: Data processing, products, and archive. *PASP* **131**, 018003

McAllister, M. et al. (2019) The evolutionary status of cataclysmic variables: eclipse modelling of 15 systems. *MNRAS* **486**, 5535

Murray, J., Warner, B., & Wickramasinghe, D. (2000) Superhumps in systems with intermediate mass ratios. *New Astron. Rev.* **44**, 51

Murray, J. R. (1998) Simulations of superhumps and superoutbursts. *MNRAS* **297**, 323

Orosz, J. A., & Bailyn, C. D. (1997a) Optical observations of GRO J1655−40 in quiescence. I. A precise mass for the black hole primary. *ApJ* **477**, 876

Orosz, J. A., & Bailyn, C. D. (1997b) Erratum: Optical observations of GRO J1655−40 in quiescence. I. A precise mass for the black hole primary. *ApJ* **482**, 1086

Osaki, Y. (1989) A model for the superoutburst phenomenon of SU Ursae Majoris stars. *PASJ* **41**, 1005

Osaki, Y., & Kato, T. (2013a) The cause of the superoutburst in SU UMa stars is finally revealed by Kepler light curve of V1504 Cygni. *PASJ* **65**, 50

Osaki, Y., & Kato, T. (2013b) Study of superoutbursts and superhumps in SU UMa stars by the Kepler light curves of V344 Lyrae and V1504 Cygni. *PASJ* **65**, 95

Osaki, Y., & Kato, T. (2014) A further study of superoutbursts and superhumps in SU UMa stars by the Kepler light curves of V1504 Cygni and V344 Lyrae. *PASJ* **66**, 15

Pala, A. F. et al. (2022) Constraining the evolution of cataclysmic variables via the masses and accretion rates of their underlying white dwarfs. *MNRAS* **510**, 6110

Patterson, J. et al. (2005) Superhumps in cataclysmic binaries. XXV. q_{crit}, $\epsilon(q)$, and mass-radius. *PASP* **117**, 1204

Ricker, G. R. et al. (2015) Transiting Exoplanet Survey Satellite (TESS). *J. of Astron. Telescopes, Instruments, and Systems* **1**, 014003

Savoury, C. D. J. et al. (2011) Cataclysmic variables below the period gap: mass determinations of 14 eclipsing systems. *MNRAS* **415**, 2025

Shingles, L. et al. (2021) Release of the ATLAS Forced Photometry server for public use. *Transient Name Server AstroNote* **7**, 1

Smak, J. I. (2006) On the mass ratio of TU Men. *Acta Astron.* **56**, 277

Smak, J., & Waagen, E. O. (2004) The 1985 superoutburst of U Geminorum. Detection of superhumps. *Acta Astron.* **54**, 433

Smith, A. J., Haswell, C. A., Murray, J. R., Truss, M. R., & Foulkes, S. B. (2007) Comprehensive simulations of superhumps. *MNRAS* **378**, 785

Stefanov, S. Y., Latev, G., Boeva, S., & Moyseev, M. (2022) Superhumps in the cataclysmic variable BG Trianguli. *MNRAS* **516**, 2775

Stellingwerf, R. F. (1978) Period determination using phase dispersion minimization. *ApJ* **224**, 953

Stolz, B., & Schoembs, R. (1984) The SU UMa star TU Mensae. *A&A* **132**, 187

Szkody, P. et al. (2007) Cataclysmic variables from Sloan Digital Sky Survey. VI. The sixth year (2005). *AJ* **134**, 185

Tonry, J. L. et al. (2018) ATLAS: A High-cadence All-sky Survey System. *PASP* **130**, 064505

Wakamatsu, Y. et al. (2021) ASASSN-18aan: An eclipsing SU UMa-type cataclysmic variable with a 3.6-hr orbital period and a late G-type secondary star. *PASJ* **73**, 1209

Warner, B. (1995) Cataclysmic Variable Stars (Cambridge: Cambridge University Press)

Whitehurst, R. (1988) Numerical simulations of accretion disks. I – Superhumps: A tidal phenomenon of accretion disks. *MNRAS* **232**, 35

Whitehurst, R., & King, A. (1991) Superhumps, resonances and accretion discs. *MNRAS* **249**, 25

Zorotovic, M., Schreiber, M. R., & Gänsicke, B. T. (2011) Post-common-envelope binaries from SDSS. XI. The white dwarf mass distributions of CVs and pre-CVs. *A&A* **536**, A42

VSOLJ
c/o Keiichi Saijo National Science Museum, Ueno-Park, Tokyo Japan

Editor Seiichiro Kiyota
e-mail:skiyotax@gmail.com